

Effects of X-ray irradiation and disk flaring on the [Ne II] 12.8 μ m emission from young stellar objects.

E. Schisano^{1,2}, B. Ercolano^{3,4}, M. Güdel⁵

¹Università degli Studi di Napoli "Federico II", Corso Umberto I, I-80138 (NA), Italy

²INAF - Osservatorio Astronomico di Capodimonte, Via Moiariello 16, I-80131 Napoli, Italy

³Institute of Astronomy, Madingley Road, Cambridge, CB3 0HA, UK

⁴Department of Physics and Astronomy, University College London, WC1E 6BT, UK

⁵Institute of Astronomy, ETH Zurich, 8093 Zurich, Switzerland

29 June 2022

ABSTRACT

The [Ne II] fine-structure emission line at 12.8 μ m has been detected in several young stellar objects (YSO) spectra. This line is thought to be produced by X-ray irradiation of the warm protoplanetary disk atmospheres, however the observational correlation between [Ne II] luminosities and measured X-ray luminosities shows a large scatter. Such spread limits the utility of this line as a probe of the gaseous phase of disks, as several authors have suggested pollution by outflows as a probable cause of the observed scatter. In this work we explore the possibility that the large variations in the observed [Ne II] luminosity may be caused instead by different star-disk parameters. In particular we study the effects that the hardness of the irradiating source and the structure (flaring) of the disk have on the luminosity and spectral profile of the [Ne II] 12.8 μ m line. We find that varying these parameter can indeed cause up to an order of magnitude variation in the emission luminosities which may explain the scatter observed, although our models predict somewhat smaller luminosities than those recently reported by other authors who observed the line with the *Spitzer* Space Telescope. Our models also show that the hardness of the spectrum has only a limited (undetected) effect on the line profiles, while changes in the flaring power of the disk significantly affect the size of the [Ne II] emission region and, as a consequence, its line profile. In particular we suggest that broad line profiles centred on the stellar radial velocity may be indicative of flat disks seen at large inclination angles.

Key words:

1 INTRODUCTION

Young solar mass stars are surrounded by $\sim 10^{-2}M_{\odot}$ of dust and gas distributed in a circumstellar disk which is the birthplace of planetary systems. In recent years efforts have been made to study the inner regions ($\lesssim 10$ AU) of these disks in order to constrain gaseous planetary system theories, and to understand the physical processes that characterise the warm and chemically active regions of protoplanetary disk atmospheres. Accurate theoretical modelling of the spectral energy distribution (SED) of young stars (see reviews by Dullemond et al. 2007 and Natta et al. 2007), coupled with observations in the near and mid-infrared carried out with the *Spitzer* Space Telescope have greatly improved our understanding of the dust component in the inner disks. On the other hand, direct studies of the gaseous component of these disks are more challenging, even though the gas exceeds the dust by over two orders of magnitude in mass. So far molecular line emission, like the CO fundamental and

overtone (Najita et al. 2007), the rovibrational transition of water (Carr et al. 2008; Salyk et al. 2008), and H₂ (Herczeg et al. 2002), have been used as diagnostics of regions with temperatures around 1000-2000 K.

The [Ne II] 12.8 μ m line (from now on [Ne II]) has been suggested as a new probe of gas in the potentially planet forming regions of the inner disks (e.g. Glassgold et al. 2007, Hollenbach & Gorti, 2009). The ionised region of the disk where this line is formed is heated mainly by X-rays from the central star (Glassgold et al. 2007, Meijerink et al. 2008, Ercolano et al. 2008a, Glassgold, Ercolano & Drake, 2009; but see also Gorti & Hollenbach, 2008). Indeed, observations from space, with the *Spitzer* Infrared Spectrometer (IRS) (Pascucci et al. 2007; Lahuis et al. 2007; Espaillat et al. 2007), and from the ground, with MICHELLE and TEXES at Gemini North (Herczeg et al., 2007; Najita et al., 2009) and VISIR at VLT (Van Boekel et al. 2009), have successfully detected the [Ne II] line in tens of young sys-

tems. The mean observed line luminosity is comparable to the predicted value from disk models, but the scatter of the observed values around this mean spans over three orders of magnitude (e.g. Güdel et al. 2009). If the [Ne II] line is to be used as a useful diagnostic of the gaseous phase of the inner disks its origins must be well understood. In particular if the line is formed in the disk by irradiation of the gas by X-rays from the central star then one naturally expects to find a correlation between line luminosity and X-ray luminosity for the observed sources. Such correlation is indeed observed (Pascucci et al 2007, Güdel et al. 2009), however, for objects with the same X-ray luminosity the [Ne II] line luminosities span over at least one order of magnitude even after removing those sources with known outflows, for which it can be argued that a large contribution to the line comes from the outflow itself (e.g. T Tau, van Boekel et al. 2009). Understanding the origin of this scatter is extremely important if useful information is to be extracted from future observations of this line. For example, one should expect that disk structural properties, like presence of holes or different degree of flaring, not considered in earlier models have an effect on the [Ne II] emitting region. Moreover, one relevant question is whether the [Ne II] line originates in the bound layers of the disk irradiated mainly by X-rays or whether it includes a contribution from a photoevaporative outflow (e.g. Alexander, 2008). In this paper we will attempt to answer the latter question by exploring the possibility that the scatter observed in [Ne II] line luminosities for a given X-ray luminosity may be due to details of the irradiating field or to the disk structure (i.e. degree of flaring). We will also produce theoretical line profiles and will compare them to available high resolution observations (e.g. Herczeg et al. 2007, Najita et al. 2009).

We use the models of Ercolano et al. (2009) to calculate [Ne II] line luminosities and line profiles for irradiating spectra of varying hardness. We also show the results from additional models that were run to investigate the effects of disk flaring on the line luminosities and profiles. The paper is organised as follows. The modeling strategy is outlined in Section 2; Section 3 contains a review of our results, while our final conclusions and discussion are given in Section 4.

2 MODELLING STRATEGY AND METHODS

We investigate the effects of two parameters on the [Ne II] emission region of protoplanetary disks: (i) hardness of the irradiating spectrum; (ii) flaring of the disk.

2.1 Hardness of the irradiating spectrum

We calculated fine structure [Ne II] line luminosities using the temperature and ionisation structure obtained by Ercolano et al. (2009) with the MOCASSIN code for EUV+X-ray irradiated protoplanetary disks. We refer to Ercolano et al. (2008a, 2009) for details of the disk models, and to Ercolano et al. (2003, 2005, 2008b) for details of the code used. The atomic database included opacity data from Verner et al. (1993) and Verner & Yakovlev (1995), energy levels, collision strengths and transition probabilities from Version 5.2 of the CHIANTI database (Landi et al. 2006, and references therein) and the improved hydrogen and helium

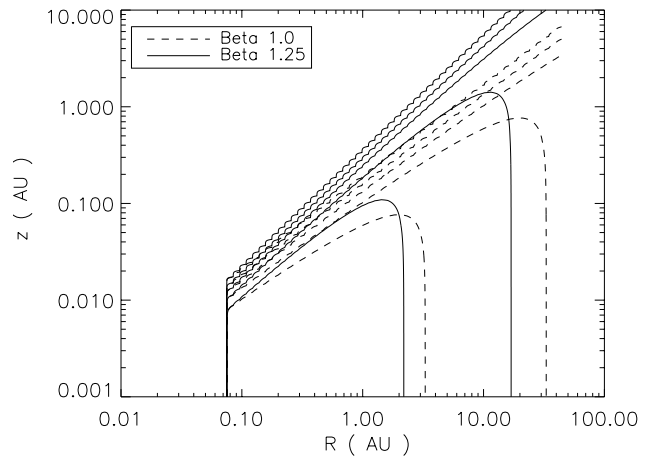


Figure 1. Isodensity curves of the two input disk models used in this work to explore the impact that different degree of flaring has on [Ne II] line luminosity. The black solid lines show the ‘flat’ model ($\beta = 1.0$) and dashed lines show the ‘flared’ model ($\beta = 1.25$). The plotted contours refer to increasing densities from 10^5 , at higher heights, to 10^{13} g cm^{-3} deeper into the disk with steps of 10^2 cm^{-3} .

free-bound continuous emission data of Ercolano & Storey (2006). In particular the Ne^+ atomic data include collisional strengths of Saraph & Tully (1994) and the transition probabilities of Blackford & Hibbert (1994). We briefly summarise here the model input parameters: we used a stellar mass of $0.7 M_{\odot}$, radius $2.5 R_{\odot}$ and effective temperature of 4000 K and an initial disk mass of $0.027 M_{\odot}$ with an outer radius of $\sim 500 \text{AU}^1$. The MOCASSIN models are coupled to a hydrostatic equilibrium routine which ensures that the effects of irradiation on the disk structure are taken into account self-consistently. Line luminosities computed without such routine result to be underestimated at worst by a factor of ~ 2 . The models were irradiated with synthetic spectra extending from the EUV to the X-ray spectral region (13.6 eV-10 keV) where the spectra were calculated using the multi-temperature plasma prescription described by Ercolano et al. (2009) and were computed using the PINTofALE IDL software suite (Kashyap & Drake 2000), adopting the solar chemical composition (Grevesse & Sauval, 1998), the atomic data from the CHIANTI compilation (Landi et al. 2006) and ion populations from Mazzotta et al. (1998). The transmittance of the synthetic spectra through neutral screens of varying thickness (as expected to be found in the circumstellar environment of pre-main sequence stars, e.g. Güdel et al., 2007, 2008) was calculated assuming neutral hydrogen column densities in the range $N_H = 10^{18} - 10^{22} \text{cm}^{-2}$, with increasing columns resulting in increasingly harder spectra, as the soft radiation is absorbed out. We present [Ne II] luminosities and line profiles for the Ercolano et al. (2009) models labeled in their work as FS0H2Lx1, FS18H2Lx1, FS19H2Lx1, FS20H2Lx1, FS21H2Lx1 and FS22H2Lx1, which consist of models irradiated by spectra screened by columns of 0., 10^{18} , 10^{19} , 10^{20} , 10^{21} , and 10^{22}cm^{-2} , and an X-ray luminosity after the screen of $L_X(0.1-10 \text{keV}) = 2 \times 10^{30} \text{erg/s}$ (“base luminosity”

¹ Note that only the inner 50 AU of the disk are considered here

hereafter; please refer to Table 1 in Ercolano et al. (2009) for a full description of the model parameters). Keeping L_X (0.1–10 keV) constant *after the screen* by normalization of the *absorbed spectrum* was done here in order to isolate the effects of the incoming radiation field hardness alone. Our prescription results in the unscreened models to have a total ionising luminosity L_{tot} (13.6 eV–10 keV) of approximately twice the X-ray luminosity and the moderately screened models ($N_H = 10^{18} \text{ cm}^{-2}$) to have a total ionising luminosity 1.2 times the base luminosity. We ran four additional models with screens of 0 and 10^{21} cm^{-2} and X-ray luminosities an order of magnitude higher and lower than the base luminosity in order to ensure that any scatter produced by varying screen thickness at fixed $L_X = 2 \times 10^{30} \text{ erg/s}$ would also be reproduced for higher or lower X-ray luminosities.

2.2 Disk Flaring

In order to investigate the effect of disk flaring on [Ne II] line luminosities, we used a simple analytical description of the disk structure, as given by Robitaille et al (2006). The density distribution is described by a fixed power-law decline of the surface density in the radial direction coupled with a gaussian relationship along the z-direction:

$$\rho(R, z) = \rho_0 \left(1 - \sqrt{\frac{R_\star}{R}} \right) \left(\frac{R_\star}{R} \right)^\alpha \exp \left(-\frac{z^2}{2h^2(R)} \right) \quad (1)$$

where ρ_0 is a scale factor fixed by the disk total mass and $h(R)$ is the disk pressure scaleheight parametrized by a power-law:

$$h(R) = h_{in} \left(\frac{R}{R_{in}} \right)^\beta \quad (2)$$

where R_{in} and h_{in} are, respectively, the dust destruction radius and the hydrostatic equilibrium scaleheight at this radius. Different values of β produce disk models with different degree of flaring, with higher β producing higher flaring. We adopted $\beta = 1.0$ and $\beta = 1.25$ to build models for a ‘flat’ and ‘flared’ disk, respectively, and we calculated the corresponding [Ne II] luminosities and line profiles. Such values are also used as limits for the β parameter in the set of SEDs of Robitaille et al. (2006), typically used in the literature to fit real observations. For either density structure we also chose R_{in} corresponding to a dust sublimation temperature of 1600 K, i.e. $R_{in} \sim 0.08 \text{ AU}$ with the previous central star parameters, $z_{factor} = 1$ from model comparison with the disk structure of Ercolano et al. (2009) and $\alpha = \beta + 1$ (Whitney et al. 2003a,b) to preserve the surface density distribution power law scaling $\Sigma(R) \sim R^{-1.5}$ of the minimum solar nebula model of Hayashi (1981). The other stellar and disk parameters were chosen to be the same as those used by the Ercolano et al. (2009) models described above.

Figure 1 shows the isodensity curves of the two disk models with different flaring powers. The flat model has a scaleheight reduced typically by a factor of about 3–4 between cylindrical radii from 1 to 10 AU when compared to the flared model. In order to isolate the effects of disk flaring only we keep the density structures fixed and do not impose hydrostatic equilibrium on these models.

2.3 Line profiles

We computed line profiles from all our models assuming Keplerian rotation at several disk inclinations. The profiles were computed by summing up the contributions from each cell which produces a Doppler broadened profile given by

$$\Phi(R, \theta, z, v) = \frac{I(R, z)}{\sqrt{2\pi}v_{th}(R, z)} \exp \left(-\frac{(v - v_{los}(R, \theta))^2}{2v_{th}(R, z)^2} \right) \quad (3)$$

where $I(R, z)$ is the power emitted by each cell and v_{th} is the local thermal velocity of the Ne^+ ions equal to

$$v_{th}(R, z) = \sqrt{\frac{3k_B T(R, z)}{m_{\text{Ne}} m_H}} \quad (4)$$

and $v_{los}(R, \theta)$ is the cell velocity projected along the line of sight. Given the temperature structure of the disk, the width of the thermal broadening in each cell is $\leq 6 \text{ km s}^{-1}$. We assumed that the midplane is optically opaque to the [Ne II] line radiation so only contributions from one side of the disk are taken into account when computing the profile. In fact, adopting the dust cross section from Weingartner and Draine 2001 of $R_V = 5.5$ extinction law, generally used to reproduce the interstellar extinction in molecular clouds, $\sigma_{12.8\mu\text{m}} = 1.6 \times 10^{-23} \text{ cm}^2 / \text{H}$ and $\sigma_{15.5\mu\text{m}} = 1.4 \times 10^{-23} \text{ cm}^2 / \text{H}$, we find that optical depths of the order of 1 are reached for hydrogen column density of about $6\text{--}7 \times 10^{22} \text{ cm}^{-2}$. Such column density are reached, for all inclination ≤ 60 , at heights of $\leq 0.1 \text{ AU}$ at a radial distance of 1 AU and $\sim 1 \text{ AU}$ at a distance of 10 AU, deeper in the disk than the Ne emitting region shown in Figure 3. In the case of almost edge-on systems the column density along the line of sight could be large enough to attenuate the observed line intensities, this is not taken into account in this work, but should be in future comparisons with real observations. Finally, we ignore scattered light contribution to the profile, which is negligible in the Weingartner & Draine (2001) dust model that has an albedo of order 0.01 at 12.8 μm , but could be significant for different dust models. The resolution of the line profiles we computed is $\lambda/\Delta\lambda \sim 150000$, since we summed all together the emission from cells whose v_{los} falls in bins wide 2 km s^{-1} . Moreover, we have convolved the line profiles with a gaussian function with FWHM of 10 km s^{-1} to degrade them to a resolution $\lambda/\Delta\lambda \sim 30000$, comparable with the high-resolution spectroscopic observations.

3 RESULTS

In this section we present the line luminosities and profiles obtained from the models described above. Monte Carlo errors on the given line luminosities were obtained by comparing multiple runs of the same model and are about 5% for the lines in question. As in Sect.2.3 we will consider the [Ne II] line luminosity response to (i) changes in the shape of the irradiating spectrum and (ii) changes in the disk density distribution (flaring).

3.1 Hardness of the irradiating spectrum

Table 1 shows the values of [Ne II] 12.8 μm and [Ne III] 15.5 μm line luminosities for models irradiated by the multi-temperature thermal spectrum of Ercolano et al. (2009)

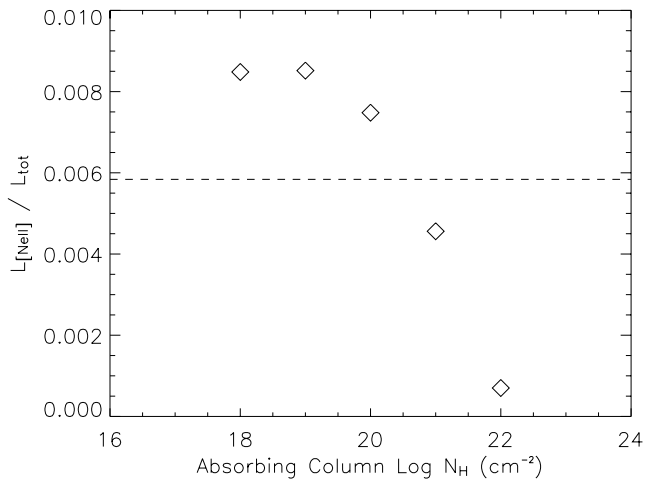


Figure 2. $L([\text{Ne II}])/L_{\text{tot}}$ as a function of the screening column of the irradiating spectrum. The dashed line indicates the value for the unscreened spectrum.

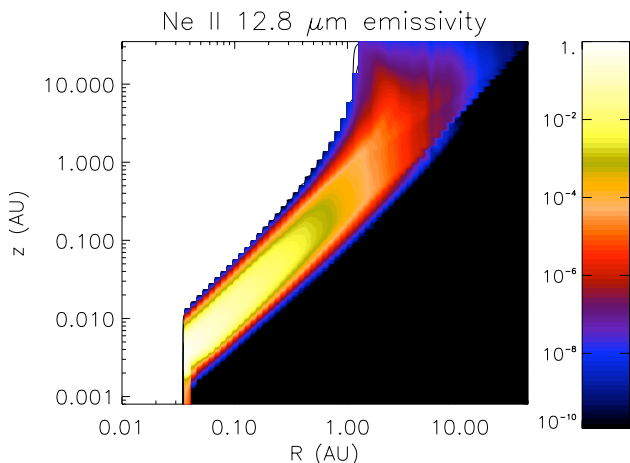


Figure 3. Two-dimensional distribution of the $[\text{Ne II}]$ emissivity in arbitrary units for a hydrostatic equilibrium disk model irradiated by an unscreened spectrum.

screened by columns of circumstellar material of thickness 0., 10^{18} , 10^{19} , 10^{20} , 10^{21} , 10^{22}cm^{-2} (see their Figure 2).

Figure 2 shows $L([\text{Ne II}])/L_{\text{tot}}$ as a function of the screening column. The dashed line indicates the value predicted in the case of unabsorbed source. From this figure and from the values in Table 1 it appears that EUV radiation is less efficient at producing $[\text{Ne II}]$ than the (soft) X-rays. In fact, even if the unscreened models have a total ionising luminosity (X-Rays+EUV) which is double than the X-ray only luminosity, they only produce a moderate increase in $L([\text{Ne II}])$. This can be easily understood when one considers that $[\text{Ne II}]$ is most efficiently produced in the low ionization layer (just above the molecular layer, see Glassgold et al., 2007; Glassgold, Ercolano & Drake, 2009), where a fast charge exchange with the abundant neutral H atoms quickly transforms most doubly ionised Ne into singly ionised. The charge exchange coefficient from singly ionised to neutral Ne is instead extremely slow, conspiring to produce high

abundance of Ne^+ in this warm layer. Instead, EUV radiation ($> 21.6\text{eV}$ and $< 100\text{eV}$) can only produce Ne^+ by standard ionisation of neutral Ne and is only efficient in the lower density upper atmosphere where an H II region like layer is formed. However, some of the Ne^+ produced in this region will be ionised to Ne^{2+} and the lower neutral H fractions in this region will result in a much less efficient charge exchange process. A spatial map of the $[\text{Ne II}]$ emission for the unscreened model is shown in Figure 3.

Furthermore, the models shown in Table 1 also suggest that the hard X-ray region is inefficient at the production of $[\text{Ne II}]$ compared with the soft X-ray region. Indeed models irradiated by hard spectra with $N_H \geq 10^{21}\text{cm}^{-2}$ show a steep decline in the $[\text{Ne II}]$ luminosity, even after forcing the X-ray luminosity (0.1-10 keV) to stay constant. This effect is dominated by the fact that models illuminated by a harder X-ray spectrum result to be colder (see discussion in Ercolano et al. 2009), the hard X-ray penetrate a region that is denser and cooler and therefore the resulting $[\text{Ne II}]$ flux is reduced. Cooler models also result in flatter disks which subtend a smaller solid angle to the source of radiation.

The hardness of the spectrum has a noticeable effect on the $[\text{Ne III}] 15.5\mu\text{m}/[\text{Ne II}] 12.8\mu\text{m}$ ratio. This ratio is higher for softer spectra due to the fact that doubly ionised Ne in these models can be produced in the upper layers of the disk where the neutral hydrogen fraction is lower and therefore charge exchange less efficient. Observations of the $[\text{Ne III}] 15.5\mu\text{m}$ (from now on $[\text{Ne III}]$) line are still rather sparse although so far low values of the $[\text{Ne III}]/[\text{Ne II}]$ ratio have been inferred (e.g. 0.06, Lahuis et al., 2007), indicating that according to our models, at least for the few objects in question, a soft (EUV-rich) irradiating spectrum is not expected.

Our results show that changes in the irradiating spectrum can give an order of magnitude scatter (an extra factor of ~ 2 is introduced when one considers that an unscreened source may contribute comparable ionising luminosity in the EUV band that would not be accounted for in the typical $L([\text{Ne II}])$ vs L_X relation).

Figure 5 (left panel) shows the surface-integrated emission for some of the models discussed in this Section. We find that in all cases half of the total $[\text{Ne II}]$ emission comes from the inner regions of the disk, $\lesssim 3\text{-}4\text{AU}$, so that the different spectra do not significantly affect the emission region for this line. Table 3 lists the half-luminosity and 90% luminosity radii for models of various screens. As the extent of the emission region does not significantly vary with spectral hardness, the line profiles obtained are also roughly invariant. As an example, in Figure 6 we show the $[\text{Ne II}]$ profile for the unscreened model seen almost face on (10° inclination) and almost edge on (80° inclination), which have Full Width Half Maximum (FWHM) of $\sim 6\text{-}8$ and $\sim 25\text{-}31\text{km s}^{-1}$ respectively.

3.2 Disk Flaring

Table 2 also shows the results for the $L([\text{Ne II}])$ for models with flared ($\beta = 1.25$) and flat ($\beta = 1.0$) disks. A casual inspection of this table reveals roughly an order of magnitude increase in the relative luminosity of the $[\text{Ne II}]$ line when the flaring is changed from $\beta = 1.0$ to $\beta = 1.25$. This is

Table 1. [Ne II] and [Ne III] luminosities of disk irradiated by different high-energetic spectrum of $L_X(0.1 - 10\text{keV}) = 2 \times 10^{30}$ erg s $^{-1}$. The disk model adopted is a d’Alessio disk model, see also Ercolano et al. 2009 for details.

MODEL	$L_{\text{tot}}(13.6 \text{ eV}-10 \text{ keV})$ $10^{30} \text{ erg s}^{-1}$	[Ne II] $(10^{28} \text{ erg s}^{-1})$	[Ne III] $(10^{28} \text{ erg s}^{-1})$
Unscreened	4.0	2.3	4.9×10^{-1}
Log $N_h = 18$	2.3	1.9	4.3×10^{-1}
Log $N_h = 19$	2.04	1.7	3.2×10^{-1}
Log $N_h = 20$	2.0	1.5	2.2×10^{-1}
Log $N_h = 21$	2.0	9.1×10^{-1}	1.5×10^{-1}
Log $N_h = 22$	2.0	1.4×10^{-1}	2.5×10^{-2}

Table 2. [Ne II] line luminosities computed at a range of L_X . The corresponding values of L_{tot} are also given.

MODEL	[Ne II] $(10^{28} \text{ erg s}^{-1})$		
$L_X [2 \cdot 10^{30} \text{ erg s}^{-1}]$	0.1	1.0	10.
Unscreened ($L_{\text{tot}} = 2 L_X$)	2.9×10^{-1}	2.3	22.0
Log(N_H)=21 ($L_{\text{tot}} = L_X$)	3.0×10^{-2}	9.1×10^{-1}	5.8
Flared ($L_{\text{tot}} = 2 L_X$)	1.0×10^{-1}	1.6	17.3
Flat ($L_{\text{tot}} = 2 L_X$)	1.7×10^{-2}	1.3×10^{-1}	7.0×10^{-1}

easily understood when considering that a more flared disk would subtend a larger solid angle to the irradiation source.

Disk flaring has also a dramatic effect on the size of the [Ne II] emitting region. Figure 4 shows two-dimensional plots of the [Ne II] emissivity for the flared and flat disk models, while the right panel of Figure 5 shows the surface-integrated emission for the line for the two disk models. As summarised in Table 3, the emission region in the flared disk model extends out to a radius of ~ 30 AU, within which 90% of the total [Ne II] luminosity is emitted. This radius is reduced to ~ 6 AU for the flat disk model. Naturally, this has consequences on the line profiles for these two cases, which are shown in Figure 7 for two disk inclinations. The FWHM for the [Ne II] line produced by a flat disk seen almost edge on (inclination 80°) is roughly 40 km s^{-1} , while it is only 17 km s^{-1} for a flared disk where the emission region extends to larger cylindrical radii. The difference is of course smaller if the disks are seen almost face on (inclination 10°), thus dominated by the contribution of the thermal broadening, where a FWHM of $\sim 10 \text{ km s}^{-1}$ is expected for a flat disk compared to a FWHM of $\sim 7 \text{ km s}^{-1}$ for a flared disk. These statistics are summarised in Table 4.

4 DISCUSSION

As the sample of observed $L([\text{Ne II}])$ luminosities from protoplanetary disks continues to grow, together with the sample of pre-main sequence stars with measured X-ray luminosities, a trend between the two quantities becomes more and more evident (Güdel et al. 2009). While this lends evidence to the [Ne II] line being a product of X-ray irradiation

Table 3. Emissivity distribution statistics. See text for details.

Model	Half-L radius (AU)	90% L radius (AU)
Unscreened	2.9	10.1
Log $N_h = 20$	3.3	13.0
Log $N_h = 21$	3.5	12.8
Log $N_h = 22$	2.9	10.1
Flared $\beta = 1.25$	12.9	34.3
Flat $\beta = 1.0$	1.5	6.1

Table 4. FWHM of the line profiles simulated for disks in Keplerian rotation viewed almost face on (10° inclination) and almost edge on (80° inclination) at two different spectral resolutions.

R =	Inclination 10 degree FWHM (km s^{-1})		Inclination 80 degree FWHM (km s^{-1})	
	150000	30000	150000	30000
Unscreened	8.2	11.1	31.3	32.6
Log $N_H = 21$	6.2	10.0	25.8	28.1
Flared $\beta = 1.25$	6.9	10.2	16.8	17.6
Flat $\beta = 1.0$	9.5	12.1	40.1	40.8

of disks as predicted by Glassgold et al. (2007), the large scatter associated with this relation makes the situation less clear-cut. For a handful of objects with known powerful outflows it is clear that this line cannot be used as a diagnostics of the gaseous *disk* phase, as the emissivities may be dominated by gas in the outflows. However, even after removing objects with known outflows from our sample we are left

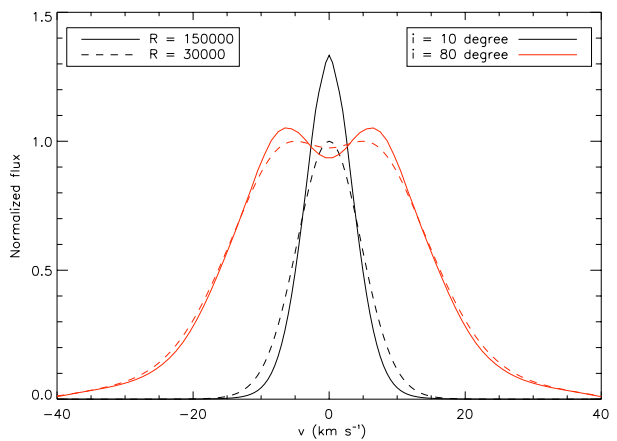


Figure 6. [Ne II] line profiles of a Keplerian disk in hydrostatic equilibrium irradiated by an unscreened EUV+X-ray source. The black lines are for low inclination ($i = 10^\circ$) and the red lines for high inclination ($i = 80^\circ$) disks. The solid lines have a resolution of $R = 150000$ and the dashed are the profiles degraded to a resolution of 30000. For clarity the lines are normalized to the peak value of the degraded case.

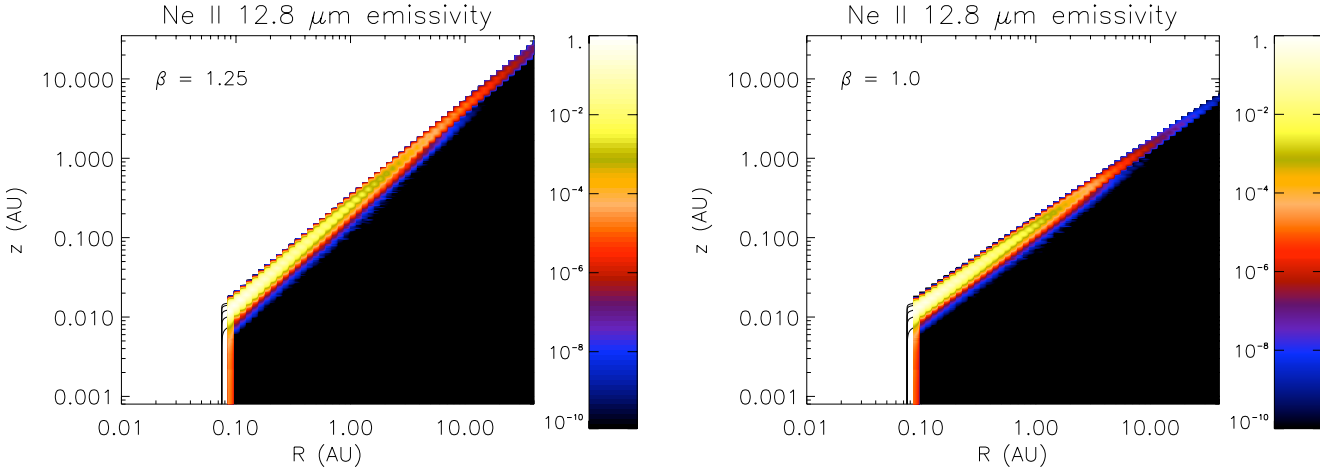


Figure 4. Two-dimensional distribution of the [Ne II] emissivity in arbitrary units. The *left* panel refers to the disk model with $\beta = 1.25$ (flared disk), instead the *right* panel show the disk model with $\beta=1.0$ (flat disk).

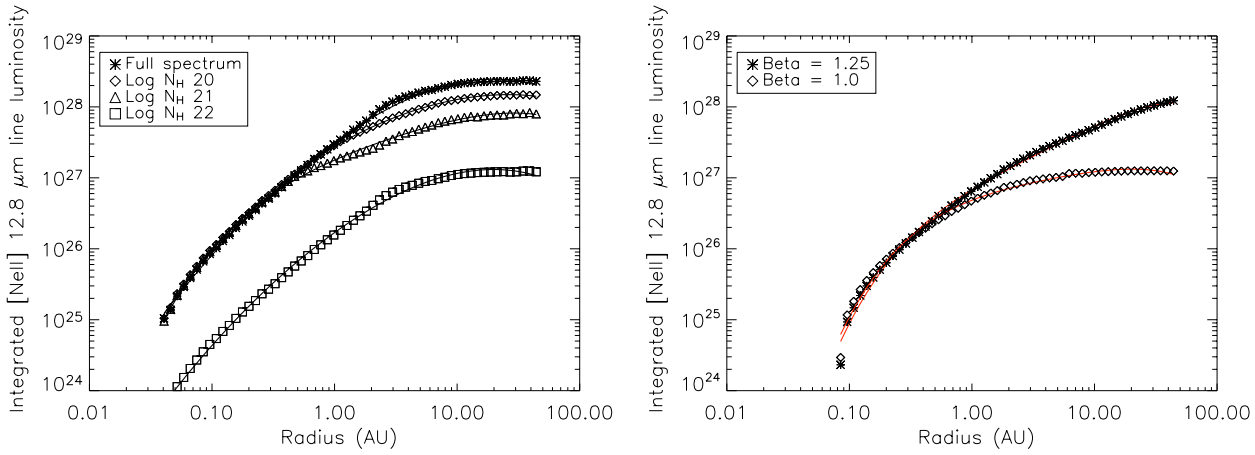


Figure 5. [Ne II] cumulative surface emission in erg s^{-1} (see text for details). *Left:* Hydrostatic equilibrium models irradiated by spectra screened by various neutral hydrogen columns. *Right:* Flat and flared disk models computed assuming Robitaille et al. (2006) density distribution.

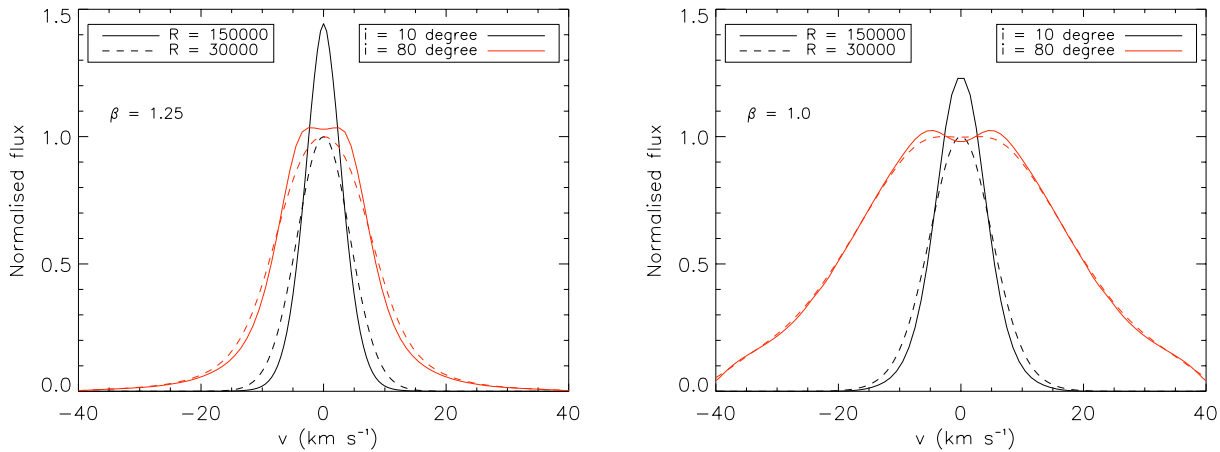


Figure 7. As in Figure 6, but for the flared disk model ($\beta = 1.25$) (*left*) and flat disk model ($\beta = 1.00$) (*right*) irradiated by an unscreened EUV+X-ray spectrum.

with approximately one order of magnitude variations in $L([\text{Ne II}])$ at any given L_X .

In this paper we have investigated the origin of the large scatter observed in the [Ne II] – L_X relation. We find that variations in the irradiating spectral shape and disk structure (flaring) are sufficient to explain the typically observed scatter of approximately one order of magnitude. Figure 8 shows the results from our models (coloured symbols) overplotted on a shaded region representing roughly the observations presented by Güdel et al. (2009), excluding the strong outflow objects (blue points in their plot). The definition of such region is affected by the limited sample statistic that does not allow a sharper outline, but it shows where the bulk of data falls. Moreover, we note here that we use luminosities *after* the screen while Güdel et al. use intrinsic luminosities derived from the observations. We have performed absorption calculations for a subset of the observations from which we found the following: absorbing the intrinsic X-ray spectral models by $N_{\text{H}} = 3 \times 10^{20} \text{ cm}^{-2} - 4.6 \times 10^{22} \text{ cm}^{-2}$ (a range occupied by the observations) reduces the 0.1-10 keV luminosity by factors of approximately 1.4–5.5 (also depending on the intrinsic thermal model from the individual fits). On average, thus, the *unabsorbed* L_X from the observations should be shifted by a factor of 3 (0.5 dex) to the left to obtain average absorbed values, with individual shifts ranging from 0.15 dex to 0.75 dex. These corrections do not change the plot qualitatively. We, however, refrain from using the individual *absorbed* (post-screen) luminosities derived from the observations here because it is not clear a priori that the absorbed luminosity seen from Earth is close to the absorbed luminosity seen by the disk. The latter luminosity is principally unknown. We also mention that Güdel et al. use the 0.3-10 keV range for their luminosities, while we use 0.1-10 keV. For the post-screen luminosities for stars with $N_{\text{H}} > 10^{20} \text{ cm}^{-2}$, however, the difference is minor.

Our model predictions seem to agree well with the observations in terms of reproducing the scatter, and at intermediate and high X-ray luminosities the absolute values of $L([\text{Ne II}])$ also roughly agree with the observations. Models with low X-ray luminosities, however, fall short of the observed values, and while detection limits can partially affect the observations, the failure of our models to produce $L([\text{Ne II}]) > 10^{28} \text{ erg/sec}$ for X-ray luminosities of $2 \times 10^{29} \text{ erg s}^{-1}$ must have another origin. Nevertheless there is an overlap between our prediction for the unabsorbed source and/or the flared disk and the shaded region. Keep in mind, however, that the correction for absorption mentioned above aggravates the discrepancy between the model predictions and the observations (the latter being moved somewhat to the left in Fig. 8), but do not have effects on the conclusions on the scatter of [Ne II] luminosities.

It would be of little use here to speculate what other observational effects may be coming into play, however one thing that is worth noticing is that the measurements plotted in the Figure all come from the *Spitzer* Space Telescope, while recent observations from the ground at higher resolution suggest often lower luminosities than the *Spitzer* data (Herczeg et al. 2007; Najita et al. 2009). This has been interpreted as possible pollution from molecular emission in the *Spitzer* band, while more recent works (Najita et al., 2009) seem to lean toward extended emission, from undetected outflows, which would contribute to the flux in the

Spitzer aperture, but would be excluded by the narrow slits used for measurements from the ground.

Our results thus support a disk origin of the observed [Ne II] emission as a consequence of X-ray irradiation, at least for systems with moderate [Ne II] luminosities and absence of jets. On the other hand, the additional parameters (X-ray spectral hardness, disk flaring) now found to influence the [Ne II] luminosity add complexity to the interpretation, and the usefulness of the [Ne II] line as a disk diagnostic depends on our ability to confine these other parameters as well. Clearly, [Ne II] *disk* diagnostics needs to avoid stars with known jets and outflows. Under the assumption of full dust and gas mixing, some information about disk flaring can be obtained by modeling the infrared spectral energy distribution (Chiang et al. 2001; Pascucci et al. 2003), providing some important constraints on the range of modeled [Ne II] luminosities. Constraining the shape of the ionizing spectrum is perhaps the most difficult task. The intrinsic spectrum can usually be modeled sufficiently well based on intermediate- or high-resolution X-ray spectroscopy, but the absorbing gas column density toward the disk may be different from that toward the observer. However, gas absorption matters the least in systems with weak or absent accretion, the possible presence of inner holes, and therefore they likely absence of strong winds emanating from the innermost disk regions. The [Ne II] *disk* diagnostic may thus be optimized for the study of transitional disks, most of which are also not known to drive outflows or jets. Several of these have been well studied, including new ground-based observations of spectrally resolved [Ne II] lines (Najita et al. 2009). In this context, the [Ne II] line may develop its full diagnostic power to study disk ionization and heating by ionizing radiation from the central star, processes that are pivotal for disk dispersal through photoevaporation (Alexander et al. 2006; Ercolano et al. 2008, 2009; Owen et al. 2009) in the first place.

High resolution and high signal-to-noise line profile can help assessing the origin of the line, with profiles centred at the stellar radial velocity being synonymous with a disk origin. This is true for all inclinations except those very close to edge on, where outflows would also produce profiles centered on the stellar radial velocity. Blue shifted profiles are expected to be observed for system with outflows observed at non edge on inclinations (e.g. Alexander, 2008), and have been recently observed by Pascucci et al. (2009) in the spectra of TW Hya, Sz 73, T Cha and CS Cha. Other examples of high resolution spectra where the line has been detected include TW Hya (Herczeg et al. 2007; $\lambda/\Delta\lambda \sim 30000$), GM Aur and AA Tau (Najita et al., 2009; $\lambda/\Delta\lambda \sim 80000$). Here the observed lines are consistent with being centred at the stellar radial velocity, suggesting a circumstellar disk origin, although the poor signal-to-noise of some of these detections makes it hard to say with certainty. The lines are broad with a FWHM of respectively ~ 21 (TW Hya), 70 (AA Tau) and 14 (GM Aur) km s^{-1} . The [Ne II] FWHM of GM Aur can be produced by a disk of normal flaring power, however the large FWHM of AA Tau requires the emission region to be dominated by very small radii and therefore implies a small degree of flaring. We finally conclude that high resolution observations of the [Ne II] line in YSOs, able to resolve its profile, are needed if this line is to be used to extract useful information on disk structure (e.g. flaring) and evolutionary

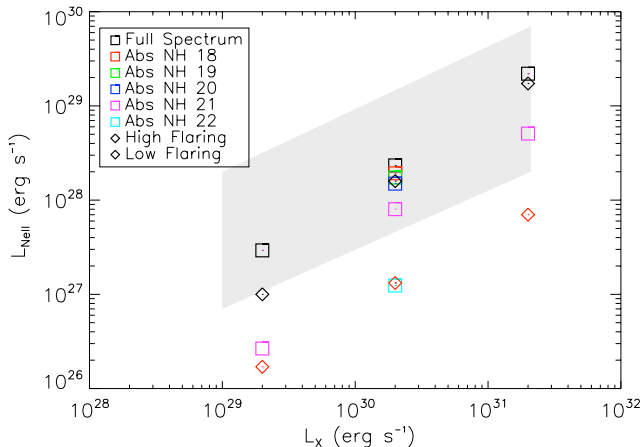


Figure 8. Comparison between the prevision of our models, where a relationship between the $L(\text{Ne II})$ and L_X is expected, and the observed system with undetected outflows (from Güdel 2008).

stage by (e.g.) the detection of outflows and photoevaporative winds by comparison with line profile models like those of Alexander (2008) or those presented in this work.

ACKNOWLEDGMENTS

We thank Juan Alcalá, Elvira Covino, Al Glassgold and Joan Najita for the useful comments. We further thank Thomas Robitaille for the information on the density structure of his disk model. This research was supported financially from INAF (PRIN 2007: *From active accretion to debris discs*).

REFERENCES

Alexander, R.D., Clarke, C.J. and Pringle, J.E., 2004, MNRAS, 354, 71
 Alexander, R.D., Clarke, C. J., Pringle, J. E, 2006, MNRAS, 369, 1, 229-239
 Alexander, R.D., 2008, MNRAS, Letters, 391, pp. L64-L68.
 Carr, J.S., Tokunaga, A.T., Najita, J., 2004, ApJ, 603, pp. 213-220.
 Carr, J. S. & Najita, J., 2008, Science, 319, 5869, pp. 504
 Chiang, E.I., Joungh, M. K., Creech-Eakman, M. J., Qi, C., Kessler, J. E., Blake, G. A., van Dishoeck, E. F., 2001, ApJ, 547, 2,1077-1089
 d'Alessio, P., Cantó, J, Calvet, N., Lizano, S., 1998, ApJ, 500, pp. 411-427
 Dullemond, C.P., Hollenbach, D., Kamp, I., d'Alessio, P., 2007 in Reipurth, B., Jewitt, D., Keil, K., eds., Protostars & Planets V. Univ. Arizona Press, Tucson, p.555
 Ercolano, B., Barlow, M.J., Storey, P.J., Liu, X.-W., 2003, MNRAS, 340, pp. 1136-1152
 Ercolano, B., Barlow, M.J., Storey, P.J., 2005, MNRAS, 362, pp. 1038-1046
 Ercolano, B., Storey, P.J., 2006, MNRAS, 372, 1875

Ercolano, B., Drake, J.J., Raymond, J.C., Clarke, C.J., 2008a, ApJ, 688, pp. 398-407
 Ercolano, B., Young, P.R., Drake, J.J., Raymond, J.C., 2008b, ApJSS, 175, pp. 534-542
 Ercolano, B., Clarke, C.J., Drake, J.J., 2009, ApJ, accepted, arXiv:0905.1001
 Espaillat, C., Calvet, N., D'Alessio, P, Bergin, E., 2007, ApJ, 664, pp. L111-L114
 Glassgold, A.E., Najita, J.R., Igea, J., 2004, ApJ, 615, pp. 972-990
 Glassgold, A.E., Najita, J.R., Igea, J., 2007, ApJ, 656, pp. 515-523.
 Glassgold, A.E., Ercolano, B., Drake, J., 2009, in prep.
 Gorti, U. and Hollenbach, D., 2008, ApJ, 615, pp. 972-990
 Grevesse and Sauval, 1998, Space Science Reviews, v. 85, pp. 161-174
 Güdel, M., Skinner, S. L., Mel'Nikov, S.Yu., Audard, M. et al., 2007, A&A, 468, pp.529-540
 Güdel, M., Skinner, S.L., Audard, M., Briggs, K.R., Cabrit, S., 2008, A&A, 478, pp.797-807
 Güdel, M., Lahuis, F., Henning, T., et al. 2009, in prep., <http://www.ipac.caltech.edu/spitzer2008/talks/ManuelGuedel.html>
 Hayashi, C. 1981, Progress of Theoretical Physics Supplement, No. 70, pp. 35-53
 Herczeg, G.J., Linsky, J.L., Valenti, J.A., Johns-Krull, C.M., Wood, B.E., 2002, ApJ, 572, pp. 310-325
 Herczeg, G.J., Najita, J.R., Hillenbrand, L.A., Pascucci, I., 2007, ApJ, 670, pp. 509-515
 Hollenbach, D. and Gorti, U., 2009, in press.
 Kashyap, V and Drake, J.J., 2000, Bulletin of the Astronomical Society of India, 28, 475
 Lahuis, F., van Dishoeck, E.F., Blake, G.A., Evans, N.J. et al., 2007, ApJ, 665, pp. 492-511
 Landi, E. and Phillips, K.J.H., 2006, ApJSS, 166, pp. 421-440
 Mazzotta, P., Mazzitelli, G., Colafrancesco, S., Vittorio, N., 1998, A&AS, 133, pp. 403-409
 Meijerink, R., Glassgold, A.E., Najita, J.R., 2008, ApJ, 676, pp. 518-531 (MGN08)
 Najita, J. R., Carr, J. S., Glassgold, A. E., Valenti, J., 2007, in Reipurth, B., Jewitt, D., Keil, K., eds., Protostars & Planets V. Univ. Arizona Press, Tucson, p.507
 Najita, J.R., Doppmann, G.W., Bitner, M.A., Richter, M.J. et al. 2009, ApJ, 697, pp. 957-963
 Natta, A., Testi, L., Calvet, N., Henning, Th., Waters, R., Wilner, D., 2007 in Reipurth, B., Jewitt, D., Keil, K., eds., Protostars & Planets V. Univ. Arizona Press, Tucson, p.555
 Owen, J., Ercolano, B., Clarke, C.J., Alexander, R.D., 2009, MNRAS, submitted
 Pascucci, I., Apai, D., Henning, Th., Dullemond, C. P. 2003, ApJ, Volume 590, Issue 2, pp. L111-L114
 Pascucci, I., Hollenbach, D., Najita, J., Muzerolle, J. et al., 2007, ApJ, 663, pp. 383-393
 Pascucci, I., Sterzik, M., 2009, ApJ, 702, pp. 724-732.
 Robitaille, T. P., Whitney, B. A., Indebetouw, R., Wood, K., and Denzmore, P. 2006, ApJS, 167, pp. 256-285
 Salyk, C., Pontoppidan, K.M.; Blake, G. A., Lahuis, F. et al. 2008, ApJ, 676, L49-52
 Weingartner and Draine 2001, ApJ, 548, 296-309
 Verner, E.M, 1993, ADNDT 55, 233
 Verner, E.M., Yakovlev, D.G., 1995, A&AS 109, 125

- Whitney, B. A., Wood, K., Bjorkman, J.E., and Wolff, M.J.
2003a, ApJ, 591, pp. 1049-1063
- Whitney, B. A., Wood, K., Bjorkman, J.E., and Cohen, M.
2003b, ApJ, 598, pp. 1079-1099
- Van Boekel, R., Güdel, M., Henning, Th., Lahuis, F.,
Pantin, E.2009, A&A, 497, pp.137-144